Ashdin Publishing
Bioceramics Development and Applications
Vol. 1 (2011), Article ID D110401, 8 pages
doi:10.4303/bda/D110401

Research Article

A Revised Replication Method for Bioceramic Scaffolds

D. Bellucci, A. Sola, and V. Cannillo

Dipartimento di Ingegneria dei Materiali e dell'Ambiente, Università Degli Studi di Modena e Reggio Emilia, Via Vignolese 905, 41125 Modena, Italy
Address correspondence to D. Bellucci, devis.bellucci@unimore.it

Received 8 April 2011; Revised 13 June 2011; Accepted 29 June 2011

Abstract Glass-ceramic macroporous scaffolds are crucial for bone tissue engineering, since they act as temporary templates for cell proliferation. An ideal scaffold should combine bioactivity, high porosity, and adequate mechanical properties. Moreover, a resistant and permeable surface is required in order to have manageable samples for both *in vitro* and *in vivo* applications. The standard replication technique usually results in relatively weak scaffolds, which can be handled with difficulty because of their brittle surfaces. For this reason, alternative preparation procedures are necessary. In this work a new protocol to realize bioceramic scaffolds is presented. The resulting samples show an original structure, which matches an external resistant surface and a highly porous internal network. In particular, the external surface, which behaves like a "shell", guarantees both high permeability and manageability. The present contribution proposes a brief description of the new protocol and a general overview of the resulting scaffolds. Moreover, some preliminary data regarding the *in vitro* bioactivity of the new scaffolds are reported.

Keywords scaffolds; bioglass; 45S5; glass-ceramics; porosity

1 Introduction

Bone replacements are frequently needed in many orthopaedic and maxillofacial surgeries. For a long time, both autografts and allografts have been considered the best treatments for bone substitutions, since they provide a fast osteointegration with the surrounding tissues after implantation. Nevertheless, they present several disadvantages. As far as allografts are concerned, there are still several issues about the possible immune rejection or disease transmission from donor; on the other hand, autografts are penalized by blood loss and donor site morbidity, which is a direct consequence of the explantation [7,24,25].

For these reasons, artificial grafts, called scaffolds, are challenging candidates for supporting the newly formed bone tissue. Scaffolds are the main ingredients for bone tissue engineering, together with harvested cells and recombinant signaling molecules [14,22]. From this point of view, the first and foremost function of a scaffold is to act as a substratum to ensure cell attachment, proliferation and differentiation. Although some properties can be specifically designed for the particular tissue to be grown, all scaffolds should meet some basic biological and structural requirements to serve this function. In particular, they must be biocompatible and they should also foster cell attachment and osteogenesis; moreover, they should posses an interconnected porous structure with a total porosity exceeding 80% and a pore size greater than 100–200 μm to allow cell penetration and vascularization; on the other hand, their mechanical strength should be sufficient to provide mechanical stability to the graft until cells synthesize the new extracellular matrix [16,17]. Finally, a resistant and permeable external surface is required in order to have manageable samples for both *in vivo* and *in vitro* applications.

Both natural and synthetic bioceramics and polymers have been employed to realize scaffolds for bone tissue repair [2,26]. From this point of view, calcium phosphate ceramics, such as hydroxyapatite or tricalcium phosphate [6,28], have been used due to their chemical and structural resemblance to the mineral phase of bone (natural apatite), which results in an excellent biocompatibility. Also bioactive silicate glasses, which were discovered by Hench in 1969 [11,12], offer remarkable advantages in terms of bioactivity, since they are able to bond to both soft and hard connective tissues. Additionally, many *in vitro* and *in vivo* studies have demonstrated that bioactive glasses regulate gene expression in both hard and soft tissue repair, although the molecular process governing the cellular response has not yet been understood fully [13,15]. The main disadvantage dealing with bioglasses is their intrinsic mechanical weakness. However, it has been observed that the most widely used bioactive glass, that is, 45S5 Bioglass® (whose proportions are 45 wt% SiO_2, 24.5 wt% CaO, 24.5 wt% Na_2O, and 6 wt% P_2O_5), is susceptible to crystallize during thermal treatment ($> 950\,^{\circ}C$), thus transforming in a bioactive and mechanically strong

crystalline phase. Thanks to this property, which enables to combine mechanical competence and bioactivity, in the last years several attempts have been made in order to employ 45S5 Bioglass® for the fabrication of scaffolds [3,8,19].

The first examples of bioceramic scaffolds for bone tissue engineering have been made by means of the polymer burning-out method [1], where organic pore formers are added to the ceramic powder. The organic phase is then removed during the thermal treatment required to sinter the ceramic phase. Unfortunately, the porosity of the obtained samples is generally low, that is, 50–60% vol., and many pores are clogged [5].

Most scaffolds based on bioactive glasses are nowadays realized by means of the foam replication method, which involves the production of ceramic foams by coating a polymeric sponge with a bioceramic slurry [4,10,27]. Then, the sponge is burned out during a proper heat treatment, which also sinters the ceramic powder. Depending on the structure of the polymeric template, this kind of scaffolds may achieve a significantly richer porosity, usually exceeding 80%. Nevertheless, such an abundant porosity is associated to a very high brittleness, which undermines the manageability of the scaffold surface [8]. For these reasons, the development of an alternative protocol is necessary.

In this work, 45S5 Bioglass®-based scaffolds were produced by means of a modified replication method, which changes some key points of the conventional *iter* and also implies the addition of polyethylene powders as porogens. The distinct feature of the new scaffolds, named "shell scaffolds", is their external surface that, like a porous shell, offers both mechanical support to the internal structure and permeability to fluids and nutrients. In the present contribution, the new protocol is discussed and the produced scaffolds are analyzed from a microstructural point of view, paying a particular attention to their porosity (content and morphology). Moreover, the bioactivity of the samples is tested preliminary by means of *in vitro* tests, where a simulated body fluid (SBF), an acellular solution with specific ionic concentrations, mimics the human extracellular fluid [18,23].

2 Materials and methods

2.1 Scaffold production

Glass-ceramic shell scaffolds were prepared from 45S5 Bioglass® powders using a polyurethane sponge as organic template.

The glass was prepared by melting the raw powder materials (commercial SiO_2, $CaCO_3$, $Na_3PO_4 \cdot 12H_2O$, Na_2CO_3 by Carlo Erba Reagenti, Italy) in a platinum crucible and then by quenching the melt in cold water. The following thermal cycle was performed: from room temperature to 1100 °C at 10 °C/min; at 1100 °C for 1 h; from 1100 °C to 1450 °C at 10 °C/min; at 1450 °C for 30 min. The melt was cast into room-temperature distilled water. The resultant frit was then ball-milled to obtain powders that were sieved below 38 μm.

The 45S5 Bioglass® slurry was obtained by dispersing the glass powders into distilled water. A polyvinylic binder (Henkel Italia S.p.A., Milano, Italy) was added to control the slurry viscosity and to favor the adhesion of the glass particles to the sponge before firing. The weight ratio of the slurry components was: 51% water, 34% 45S5 Bioglass®, 10% polyvinylic binder, and 5% polyethylene powder (particle size between 90 and 150 μm, Goonvean Fibres, UK). The latter was added as an additional pore former.

Then the sponge blocks were manually immersed into the slurry for 30 s and accurately impregnated. The sponges were retrieved from the suspension and, unlike the traditional replication technique, they were not squeezed but kept fully loaded with the slurry. The samples (green bodies) were immediately dried using an air flux at 150 °C for 20 minutes.

This procedure represents an innovation with respect to the traditional replication method. In fact, the conventional approach implies that

(1) the green bodies are usually squeezed before drying, in order to remove the exceeding slurry;
(2) the green bodies are slowly dried.

Instead, in the new protocol the samples were kept fully loaded with the slurry during both the retrieving and the drying steps. Moreover, the addition of the polyethylene particles to the slurry helped to increase and control the final porosity, especially on the sample surface.

Post-forming thermal treatments were performed to burn out the organic phase and sinter the 45S5 Bioglass® structure. With this aim, the samples were introduced into a furnace at room temperature and heat-treated at 1050 °C for three hours [8].

A flowchart of the new protocol is reported in Figure 1, together with a sketch of the traditional replication method.

2.2 Scaffold characterization

The microstructure of the resulting scaffolds was qualitatively investigated in a scanning electron microscope, SEM (ESEM Quanta 2000, FEI Co., Eindhoven, The Netherland), before and after soaking in SBF, in order to observe the degree of sintering and the pore size, morphology, distribution, and interconnection. The instrument was operated in low-vacuum mode, with a pressure of 0.5 Torr. The chemical analyses were performed by X-ray Energy Dispersion Spectroscopy, EDS (Inca, Oxford Instruments, Buckinghamshire, UK), in order to evaluate the hydroxyapatite formation on the samples surface after soaking in SBF.

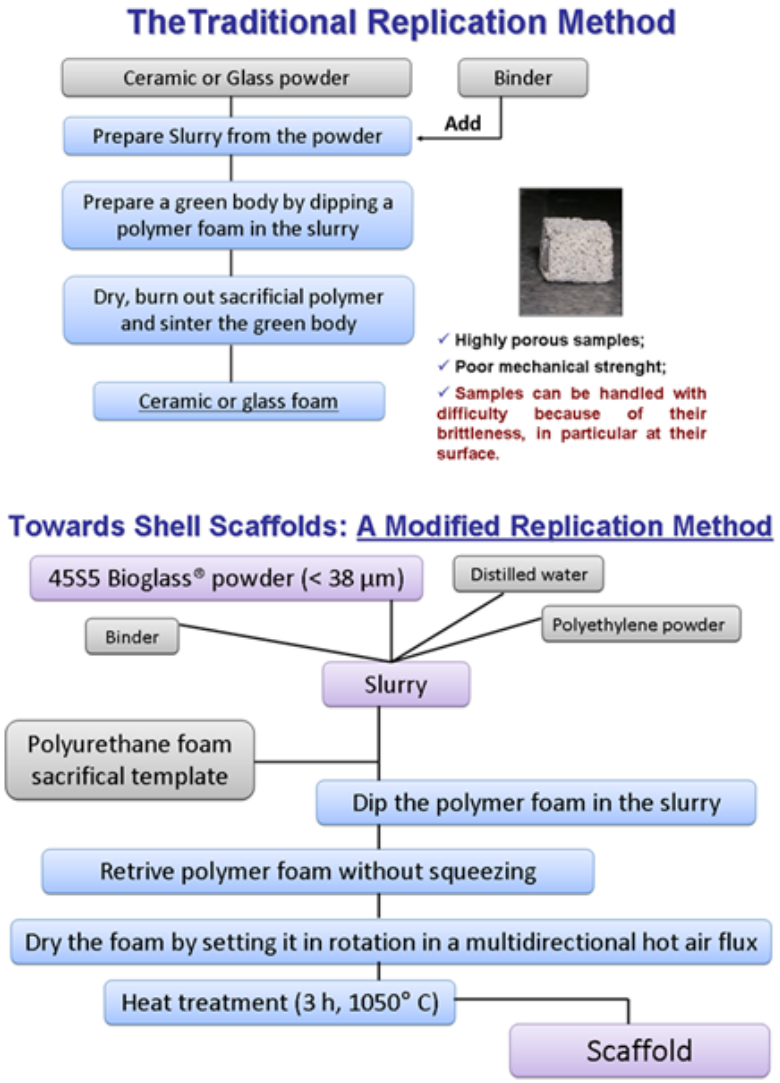

Figure 1: Flowcharts of the traditional replication method and of the modified replication method employed to produce shell scaffolds.

The scaffolds were also characterized by means of X-ray diffraction (XRD) with the aim to investigate the eventual devetrification of the 45S5 Bioglass® after sintering. The samples were ground into a powder and then analyzed by means of a PANalytical X'pert PRO diffractometer employing a Cu kα radiation (PANalytical, Almelo, the Netherlands). Data were collected in the angular range 10°–70° 2θ with steps of 0.017° and a step time of 52.8 s.

The total pore content (% vol.) of the scaffolds was calculated by

$$P_{\%} = \left(1 - \frac{W_f}{W_0}\right) \times 100,$$

where $P_{\%}$ is the total pore content (expressed in vol.%), W_f is the measured weight of the scaffold, and W_0 is the theoretical one, obtained by multiplying the 45S5 Bioglass® density $\rho = 2.7\,\mathrm{g/cm^3}$ [21] by the scaffold volume. An image analysis was also performed with the aim to investigate more carefully the porosity. SEM images of the scaffolds were acquired with a proper magnification (X500); the contrast of the pictures was emphasized in order to identify the pores more easily. Afterwards, the images were analyzed by means of an open-source software (ImageJ) and the mean porosity was calculated. Four different samples were considered and five micrographs were acquired on each of them, in order to have statistical data.

The assessment of the scaffold bioactivity was carried out using the standard *in vitro* protocol developed by Kokubo et al. [18]. In fact, in order to mimic *in vitro* the possible formation of hydroxyapatite onto the scaffolds, the samples were immersed in flasks containing 20 mL of SBF and maintained at a controlled temperature of

37 °C. Samples were extracted from the SBF after given times of 3, 7, and 14 days. A periodic refresh of the SBF (every 48 hours) was used to simulate the circulation in the human body. Once extracted from the solution, the samples were rinsed with deionized water and left to dry at room temperature.

3 Results and discussion

Shell scaffolds with different shape are presented in Figure 2. Figure 3 reports a digital camera image of the samples, with a particular focus on their surface. At the center of the picture, the "outer shell" of the scaffold was intentionally broken to reveal the internal structure. A particular attention should be paid to the relevant difference existing between the internal network of pores, resembling the original sponge structure, and the outer shell, characterized by a typical "grid" morphology, with large voids separated by thick walls, that confers permeability and manageability at the same time. In spite of this structural difference, it is possible to appreciate the excellent connection between the outer and the inner parts of the samples. In particular, the outer network of macropores and strong struts, resembling the bone trabecolae, behaves as a support for the internal sponge-like structure. The presence of this peculiar external surface inspired the name of these new "shell scaffolds".

Micrographs of the scaffolds are reported in Figure 4. It is possible to observe the open and interconnected macroporosity, resembling the original sponge network, which is essential to allow cell penetration and mechanical interlocking between the scaffold and the surrounding bone tissue. The pore sizes mainly fall within the 200–500 μm range. All the proposed samples are also characterized by a widespread microporosity, which derives from the decomposition gases generated by the burning out of the organic phase, resulting in a very rough surface of the struts. An adequate microporosity is crucial in order to promote the diffusion of fluids and nutrients by means of capillarity in-growth; on the other hand, a rough surface is an ideal texture to foster the absorption of biological metabolites and the cell attachment [9]. Details of the sample microstructure are reported in Figure 5. It should be noted that an excellent sintering level was obtained and the struts between pores are well densified.

The average porosity of the scaffolds, resulting from density measurements, is not lower than 80% vol.; this value, which was further confirmed by the image analysis, satisfies the requirements to foster the infiltration of progenitor cells and vascularization [16, 17]. Furthermore, the internal porosity is expected to be even higher than the calculated value, since in these samples most of the glass coats the external surface. The porosity value for the presented samples is among the highest ones described in the literature for scaffolds realized by means of the replication technique [8]. The increased porosity is the result of the addition of polyethylene particles, which act as porogens.

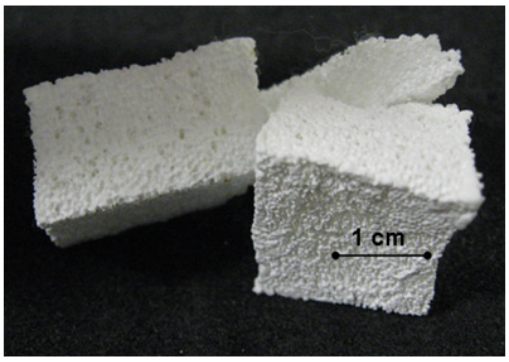

Figure 2: 45S5 Bioglass® shell scaffolds.

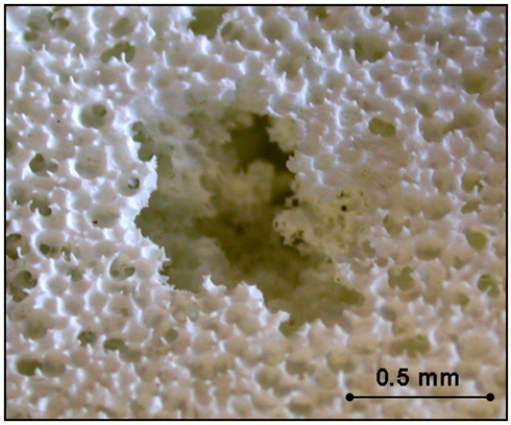

Figure 3: Digital camera image of a representative shell scaffold.

As already mentioned, thanks to their original structure, characterized by a rich internal porosity coupled with a compact but highly permeable external surface, resembling a shell, the scaffolds presented in this work can be named "shell scaffolds". If required, the porosity can be further increased and optimized by adding the organic pore former in proper amounts, making the developed protocol rather versatile. It is important to stress that the new shell scaffolds can be easily handled with no damage, while samples realized by means of the conventional replication method are usually brittle.

The structural strength and good manageability of the samples may also benefit form the devetrification promoted by the thermal treatment. As revealed by the XRD graphs presented in Figure 6, the glass widely crystallized, with a prevalent development of $Na_6Ca_3Si_6O_{18}$, which is frequently reported in the literature on 45S5 Bioglass®-based scaffolds [19].

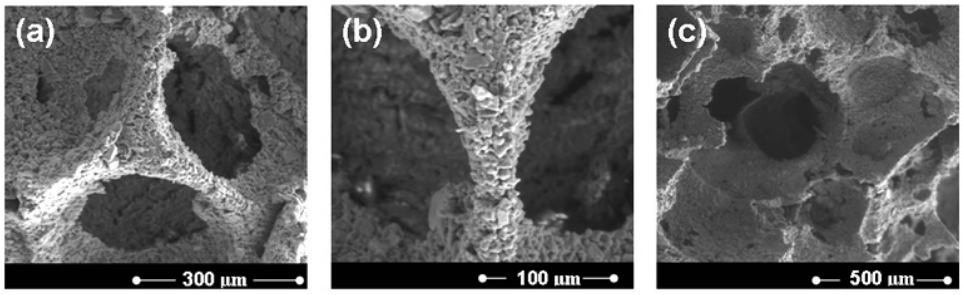

Figure 4: Scanning electron micrographs of the shell scaffolds internal structure.

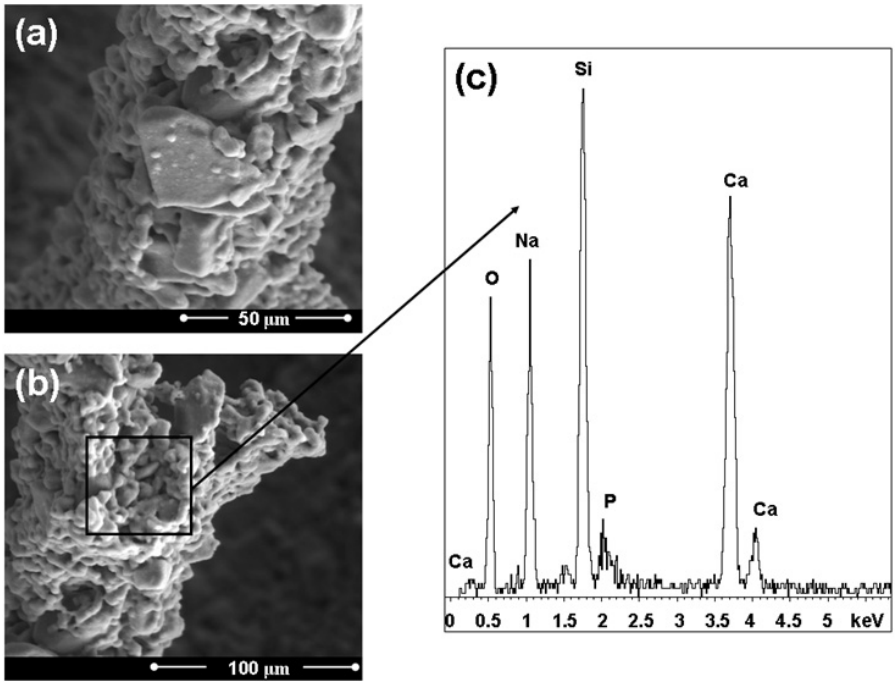

Figure 5: Scanning electron micrographs of the internal structure of the shell scaffolds: details of the struts at different magnifications (a), (b); EDS results of the analysis carried out on the outlined area (c).

The bioactivity of the shell scaffolds was evaluated by means of *in vitro* tests, that is, by immersing them in SBF for different periods, from 3 to 14 days. Indeed, a crucial preliminary requirement for the *in vivo* biointegration of the scaffolds is the *in vitro* formation of a hydroxyapatite layer. According to Boccaccini et al. [3], who based their considerations on the model originally developed by Hench and coworkers to describe the hydroxyapatite precipitation and crystallization on the surface of bioactive glasses [11], the 45S5 Bioglass®-derived glass-ceramics start their dissolution in SBF by exchanging alkali or alkaline-earth cations, such as Na^+ or K^+, with H^+ or H_3O^+ ions from the physiological solution (ion leaching). This phenomenon results in a breakdown and amorphization of the crystalline structure by point defects produced during the ion exchange. At the same time, silanol groups (Si–OH) form at the sample/solution interface, and their subsequent rearrangement and polycondensation produce a silica gel layer on the sample surface. Micrographs of the scaffold surface after 3 days in SBF are reported in Figure 7. White spherical agglomerates, with the typical morphology of the hydroxyapatite developed in SBF, covered the sample surface. In particular, both the external shell and the internal structure of the scaffold were clothed in hydroxyapatite precipitates. As shown in Figure 6, the XRD performed on the crushed sample could not detect the hydroxyapatite phase revealed by the SEM observation. It is likely that the HA presence was not rich enough after just 3 days in SBF to be perceivable by the diffraction technique. On the other hand, it is reasonable that even the strongest peaks of HA, which are located in the 30°–32° 2θ range, could be hidden by the $Na_6Ca_3Si_6O_{18}$ signals. However, as a general trend, the intensity of the $Na_6Ca_3Si_6O_{18}$ peaks

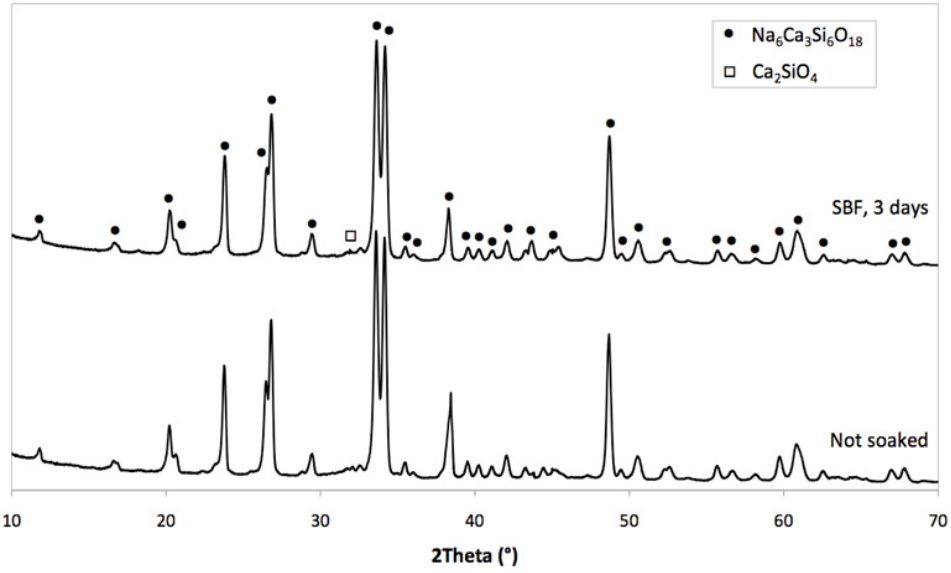

Figure 6: XRD spectra of shell scaffolds before and after 3-day soaking in SBF (diffractograms acquired on crushed samples).

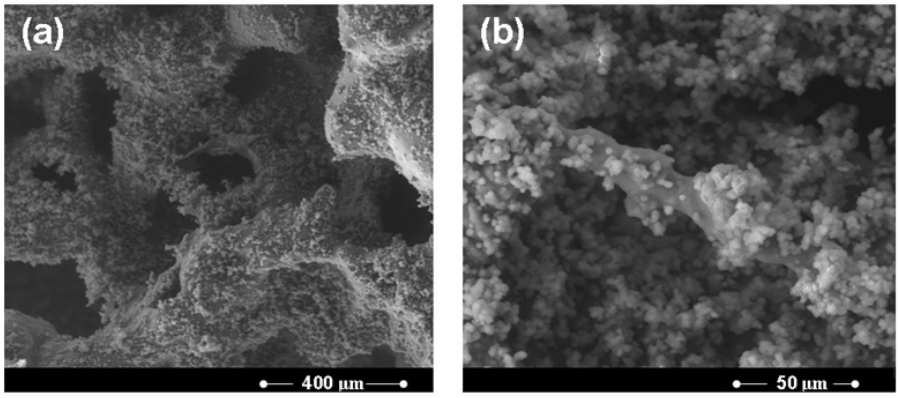

Figure 7: Micrograph of the shell scaffold internal structure after immersion in simulated body fluid for 3 days.

decreased after 3 days in SBF. This may be associated to the amorphization of the silicate phase, which represents the first step towards the hydroxyapatite formation [3].

Increasing the soaking time to 14 days, the hydroxyapatite layer fully coated the entire surface (Figure 8). The EDS analysis performed in the reported area of Figure 8(b) shows the presence of Ca and P in proportion similar to that in hydroxyapatite, since the Ca/P ratio is about 1.7, while in the stoichiometric hydroxyapatite it is 1.67 [20]. The presence of Si is due to the silica gel layer underneath the precipitates. As a term of comparison, the EDS analysis of the sample surface before soaking in SBF is reported in Figure 5(c).

The development of a hydroxyapatite layer, which progressively grows on both the external surface and internal pore struts of the scaffold, represents the preliminary step towards the bone integration. Therefore, a bioactive behavior of the shell scaffolds should be expected also *in vivo*.

4 Conclusions and perspectives

A new approach to realize bioceramic scaffolds for bone tissue repair and regeneration has been discussed. The produced samples, named “shell scaffolds”, are characterized by a compact and at the same time permeable surface which surrounds and supports a highly porous internal network, resembling the bone structure. For these reasons, the new protocol goes beyond the limits of the traditional replication method, by which brittle samples are often produced. Moreover, it is possible to increase, if necessary, the scaffold porosity and the surface permeability by increasing the amount of thermally removable organic phase to the slurry the polyurethane sponges are soaked in.

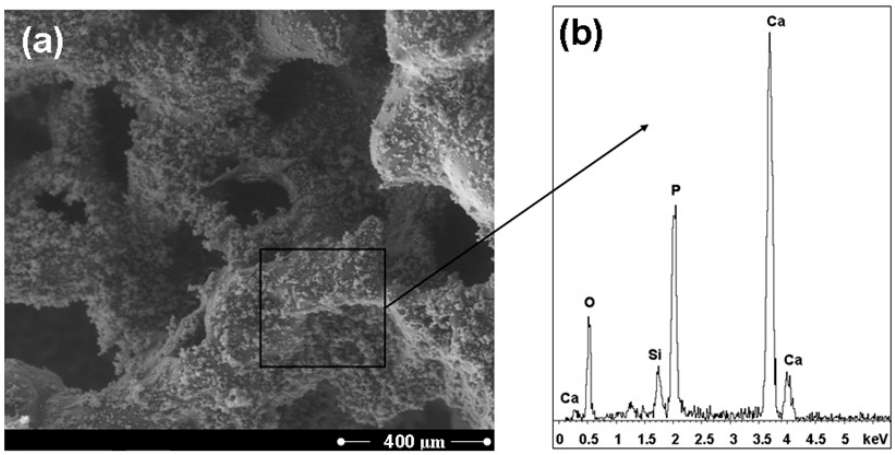

Figure 8: Micrograph of the shell scaffold internal structure after immersion in simulated body fluid for 14 days (a); EDS results of the analysis carried out on the outlined area (b).

The bioactivity of the shell scaffolds was tested *in vitro* by immersing them in a simulated body fluid. HA agglomerates were observed diffusedly on the sample surface already after three days in SBF. From this point of view, it will be interesting to perform biological tests employing osteoblasts in a biological reactor. These studies will be the subject of future works.

References

[1] D. Bellucci, V. Cannillo, A. Sola, F. Chiellini, M. Gazzarri, and C. Migone, *Macroporous Bioglass®-derived scaffolds for bone tissue regeneration*, Ceram Int, 37 (2011), 1575–1585.

[2] J. J. Blaker, V. Maquet, R. Jérôme, A. R. Boccaccini, and S. N. Nazhat, *Mechanical properties of highly porous PDLLA/Bioglass® composite foams as scaffolds for bone tissue engineering*, Acta Biomater, 1 (2005), 643–652.

[3] A. R. Boccaccini, Q. Chen, L. Lefebvre, L. Gremillard, and J. Chevalier, *Sintering, crystallisation and biodegradation behaviour of Bioglass®-derived glass-ceramics*, Faraday Discuss, 136 (2007), 27–44.

[4] O. Bretcanu, C. Samaille, and A. R. Boccaccini, *Simple methods to fabricate Bioglass®-derived glass-ceramic scaffolds exhibiting porosity gradient*, J Mater Sci Mater Med, 43 (2008), 4127–4134.

[5] C. V. Brovarone, E. Verné, and P. Appendino, *Macroporous bioactive glass-ceramic scaffolds for tissue engineering*, J Mater Sci Mater Med, 17 (2006), 1069–1078.

[6] E. Charriére, J. Lemaitre, and P. Zysset, *Hydroxyapatite cement scaffolds with controlled macroporosity: fabrication protocol and mechanical properties*, Biomaterials, 24 (2003), 809–817.

[7] Q. Chen, J. A. Roether, and A. R. Boccaccini, *Tissue engineering scaffolds from bioactive glass and composite materials*, in Topics in Tissue Engineering, N. Ashammakhi, R. Reis, and F. Chiellini, eds., vol. 4, 2008.

[8] Q. Z. Chen, I. D. Thompson, and A. R. Boccaccini, *45S5 Bioglass®-derived glass-ceramic scaffolds for bone tissue engineering*, Biomaterials, 27 (2006), 2414–2425.

[9] D. D. Deligianni, N. D. Katsala, P. G. Koutsoukos, and Y. F. Missirlis, *Effect of surface roughness of hydroxyapatite on human bone marrow cell adhesion, proliferation, differentiation and detachment strength*, Biomaterials, 22 (2001), 87–96.

[10] Q. Fu, M. N. Rahaman, B. S. Bal, R. F. Brown, and D. E. Day, *Mechanical and in vitro performance of 13–93 bioactive glass scaffolds prepared by a polymer foam replication technique*, Acta Biomater, 4 (2008), 1854–1864.

[11] L. L. Hench, *Bioceramics: from concept to clinic*, J Am Ceram Soc, 74 (1991), 1487–1510.

[12] L. L. Hench, *The story of Bioglass®*, J Mater Sci Mater Med, 17 (2006), 967–978.

[13] L. L. Hench, *Genetic design of bioactive glass*, J Eur Cer Soc, 29 (2009), 1257–1265.

[14] Y. Ikada, *Tissue Engineering, Volume 8: Fundamentals and Applications*, Academic Press, New York, 1st ed., 2006.

[15] G. Jell and M. M. Stevens, *Gene activation by bioactive glasses*, J Mater Sci Mater Med, 17 (2006), 997–1002.

[16] J. R. Jones and A. R. Boccaccini, *Cellular ceramics in biomedical applications: tissue engineering*, in Cellular Ceramics: Structure, Manufacturing, Processing and Applications, M. Scheffler and P. Colombo, eds., Wiley-VCH Verlag GmbH & Co. KgaA, Weinheim, Germany, 2005, 550–573.

[17] V. Karageorgiou and D. Kaplan, *Porosity of 3D biomaterial scaffolds and osteogenesis*, Biomaterials, 26 (2005), 5474–5491.

[18] T. Kokubo and H. Takadama, *How useful is SBF in predicting in vivo bone bioactivity?*, Biomaterials, 27 (2006), 2907–2915.

[19] L. Lefebvrea, J. Chevaliera, L. Gremillard, R. Zenatib, G. Tholleta, D. Bernache-Assolant, et al., *Structural transformations of bioactive glass 45S5 with thermal treatments*, Acta Mater, 55 (2007), 3305–3313.

[20] H. Liu, H. Yazici, C. Ergun, T. J. Webster, and H. Bermek, *An in vitro evaluation of the Ca/P ratio for the cytocompatibility of nano-to-micron particulate calcium phosphates for bone regeneration*, Acta Biomater, 4 (2008), 1472–1479.

[21] S. Lopez-Esteban, E. Saiz, S. Fujino, T. Oku, K. Suganuma, and A. P. Tomsia, *Bioactive glass coatings for orthopedic metallic implants*, J Eur Cer Soc, 23 (2003), 2921–2930.

[22] P. X. Ma, *Scaffolds for tissue fabrication*, Materials Today, 7 (2004), 30–40.

[23] D. Rohanová, A. R. Boccaccini, D. M. Yunos, D. Horkavcová, I. Březovská, and A. Helebrant, *TRIS buffer in simulated body fluid distorts the assessment of glass-ceramic scaffold bioactivity*, Acta Biomater, 7 (2011), 2623–2630.

[24] A. J. Salgado, O. P. Coutinho, and R. L. Reis, *Bone tissue engineering: state of the art and future trends*, Macromol Biosci, 4 (2004), 743–765.

[25] C. G. Simon Jr., C. A. Khatri, S. A. Wight, and F. W. Wang, *Preliminary report on the biocompatibility of a moldable, resorbable, composite bone graft consisting of calcium phosphate cement and poly(lactide-co-glycolide) microspheres*, J Orthop Res, 20 (2002), 473–482.

[26] C. Vitale-Brovarone, F. Baino, and E. Verné, *High strength bioactive glass-ceramic scaffolds for bone regeneration*, J Mater Sci Mater Med, 20 (2009), 643–653.

[27] C. Vitale-Brovarone, E. Verné, L. Robiglio, P. Appendino, F. Bassi, G. Martinasso, et al., *Development of glass-ceramic scaffolds for bone tissue engineering: characterisation, proliferation of human osteoblasts and nodule formation*, Acta Biomater, 3 (2007), 199–208.

[28] M. C. von Doernberg, B. von Rechenberg, M. Bohner, S. Grünenfelder, G. H. van Lenthe, R. Müller, et al., *In vivo behavior of calcium phosphate scaffolds with four different pore sizes*, Biomaterials, 27 (2006), 5186–5198.